

# Eliminating Polar Singularities in Global Wave Models

**Adrean Webb**

*Institute of Science Tokyo*  
[webb@phys.sci.isct.ac.jp](mailto:webb@phys.sci.isct.ac.jp)

**Baylor Fox-Kemper**

*Brown University*  
[baylor@brown.edu](mailto:baylor@brown.edu)

**Natasha Flyer**

*University of Colorado Boulder*  
[natasha.flyer@gmail.com](mailto:natasha.flyer@gmail.com)

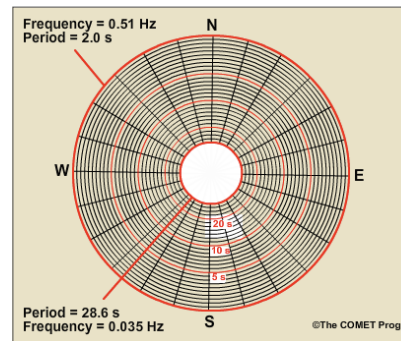
## I. Introduction

- Global third-generation spectral wave models use a governing equation in  $2D \times 2D$  phase space that contains polar singularities in both the spatial and spectral domains.
- Singularities can be circumvented using artificial boundaries or advanced model setups (e.g., structured multi-cell, curvilinear grids).
- However, polar singularities are not inevitable, and a non-singular global wave model can be constructed in  $3D \times 3D$  phase space.

**Spatial**



**Spectral**



- At the poles, spatial coordinates are non-unique and spectral directions are undefined.

## II. Polar singularities in 4D phase space

- For simplified kinematic testing, consider an aqua planet without source terms, ocean currents, or bathymetric variations.
- A  $2D \times 2D$  form of the wave action balance (WAB) equation, using a spatial global Mercator projection and a spectral global tangent plane projection, can be written as:

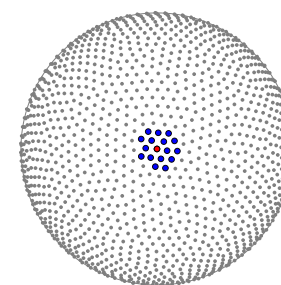
$$\left\{ \partial_t + \frac{c_g(f)}{R_E} \left( \frac{\cos \theta}{\cos \mu} \partial_\lambda + \sin \theta \partial_\mu - \tan \mu \cos \theta \partial_\theta \right) \right\} \mathcal{W}(\lambda, \mu, f, \theta, t) = 0$$

- $\mathcal{W}$  : wave action density
- $(\mu, \lambda)$  : latitude and longitude
- $R_E$  : radius of the Earth

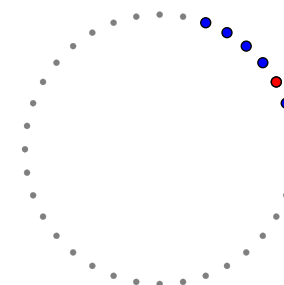
## V. Numerical method and directional alignment

- Approach tested with RBF-FD, a finite difference method on unstructured nodes.
- Directional alignment of the nearest neighbors is defined by their projection onto the local tangent plane for the stencil node.
- PHS+Poly scheme is used to avoid parameter tuning and add stability near boundaries.
- Differential weights are assembled per spatial and directional node using nearest neighbors.
- Wave spectral density for the desired projected direction is interpolated at each neighbor to estimate spatial advection in the same fixed direction.

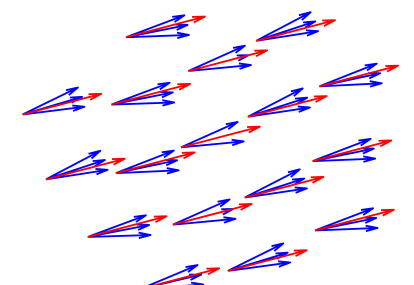
**Spatial stencil**



**Directional stencil**

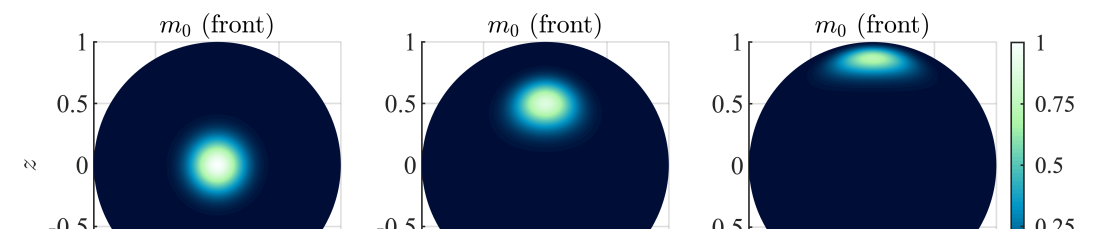


**Interpolated direction**



## VI. Results: Propagation across North Pole

- Initial spatial amplitude: Normalized Gaussian bell (half-width  $20^\circ$ ) centered at  $(1,0,0)$ .
- Initial spectral distribution: Narrow cosine-power distribution (exponent = 20,  $\approx 60^\circ$  width) with an initial dominant direction of  $(0,0,1)$  at spatial bell center.



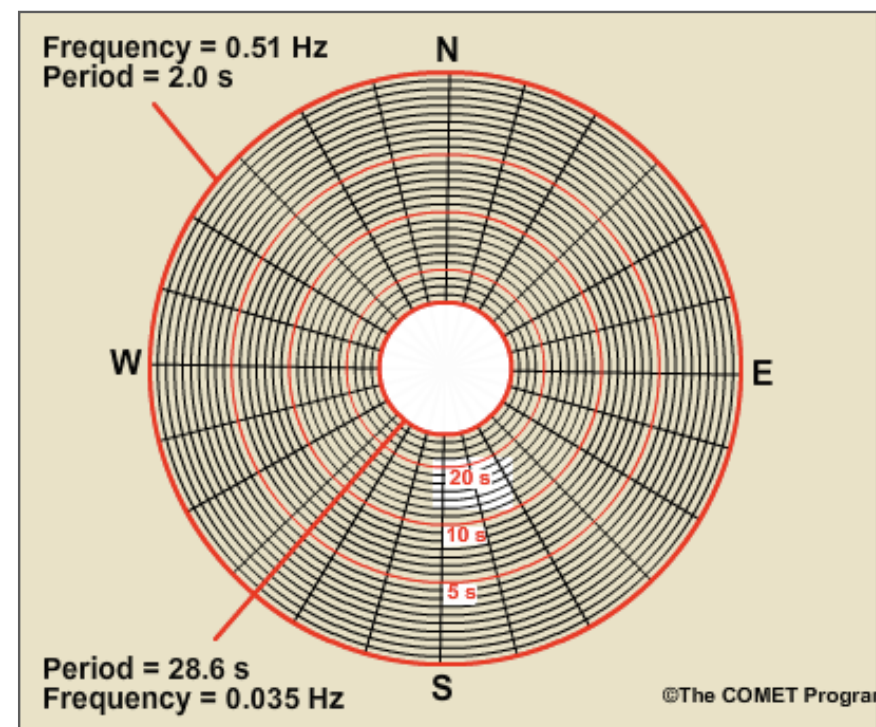
# I. Introduction

- Global third-generation spectral wave models use a governing equation in  $2D \times 2D$  phase space that contains polar singularities in both the spatial and spectral domains.
- Singularities can be circumvented using artificial boundaries or advanced model setups (e.g., structured multi-cell, curvilinear grids).
- However, polar singularities are not inevitable, and a non-singular global wave model can be constructed in  $3D \times 3D$  phase space.

**Spatial**



**Spectral**



- At the poles, spatial coordinates are non-unique and spectral directions are undefined.

## II. Polar singularities in 4D phase space

- For simplified kinematic testing, consider an aqua planet without source terms, ocean currents, or bathymetric variations.
- A  $2D \times 2D$  form of the wave action balance (WAB) equation, using a spatial global Mercator projection and a spectral global tangent plane projection, can be written as:

$$\left\{ \partial_t + \frac{c_g(f)}{R_E} \left( \frac{\cos \theta}{\cos \mu} \partial_\lambda + \sin \theta \partial_\mu - \tan \mu \cos \theta \partial_\theta \right) \right\} \mathcal{W}(\lambda, \mu, f, \theta, t) = 0$$

- $\mathcal{W}$  : wave action density
- $(\mu, \lambda)$  : latitude and longitude
- $R_E$  : radius of the Earth
- $c_g$  : deep-water group velocity
- $(f, \theta)$  : frequency and direction
- Notice that there are transitions across the poles (e.g., at the North Pole, the coordinates shift as  $\lambda \Rightarrow \lambda + 180^\circ$ ,  $\mu \Rightarrow 180^\circ - \mu$ , and  $\theta \Rightarrow -90^\circ$ ).

## III. Non-singular approach using full 6D phase space

- To avoid introducing singularities from 2D projection mappings, the full 3D spatial and spectral domains are preserved while restricting transport to the relevant 2D manifolds.

### III. Non-singular approach using full 6D phase space

- To avoid introducing singularities from 2D projection mappings, the full 3D spatial and spectral domains are preserved while restricting transport to the relevant 2D manifolds.
- Ensures that each spatial position and spectral direction remains unique without increasing the number of model unknowns.
- Proposed solution (for a general dispersion relation  $\Omega$ ) is of the form

$$\begin{aligned} \partial_t \mathcal{W}(\mathbf{x}, \mathbf{k}, t) + P_{\mathbf{k}} \nabla_{\mathbf{k}} \Omega(\mathbf{x}, \mathbf{k}, t) \cdot P_{\mathbf{x}} \nabla_{\mathbf{x}} \mathcal{W}(\mathbf{x}, \mathbf{k}, t) \\ - P_{\mathbf{x}} \nabla_{\mathbf{x}} \Omega(\mathbf{x}, \mathbf{k}, t) \cdot P_{\mathbf{k}} \nabla_{\mathbf{k}} \mathcal{W}(\mathbf{x}, \mathbf{k}, t) = 0 \end{aligned}$$

where  $P_{\mathbf{x}}$  and  $P_{\mathbf{k}}$  act as projection operators for the spatial and spectral domains.

- Following restriction is imposed to ensure the spatial and spectral coordinates are tangent:

$$\mathbf{x} \cdot \mathbf{k} = 0, \quad \text{for } \mathbf{x}, \mathbf{k} \in \mathbb{R}^3$$

### IV. Spherical projection operator

- Spherical projection operator is used to (i) confine spatial advection to the sphere and (ii)



$$\mathbf{x} \cdot \mathbf{k} = 0, \quad \text{for } \mathbf{x}, \mathbf{k} \in \mathbb{R}^3$$

## IV. Spherical projection operator

- Spherical projection operator is used to (i) confine spatial advection to the sphere and (ii) confine spectral evolution to the plane tangent to the spatial location.

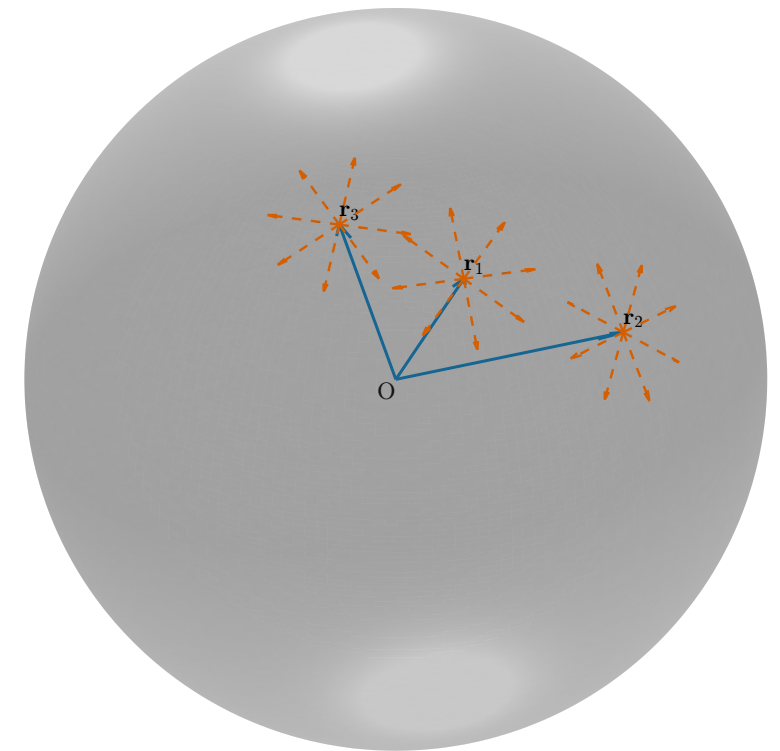
- For any  $\boldsymbol{\nu} \in \mathbb{R}^3$ , we define  $P_{\mathbf{x}}$  (and  $P_{\mathbf{k}}$  similarly) as

$$P_{\mathbf{x}} \boldsymbol{\nu} = \boldsymbol{\nu} - \hat{\mathbf{n}} (\hat{\mathbf{n}} \cdot \boldsymbol{\nu}) = \left( \mathbf{I}_3 - \frac{1}{R_E^2} \mathbf{x} \mathbf{x}^T \right) \boldsymbol{\nu}$$

- In the kinematic test case, the proposed solution simplifies (surprisingly\*) to the set of decoupled equations

$$\left\{ \partial_t + \mathbf{c}_g(\mathbf{k}) \cdot \nabla_{\mathbf{x}} \right\} \mathcal{W}(\mathbf{x}, \mathbf{k}, t) = 0$$

for each  $\mathbf{k} \in \mathbb{R}^3$  that satisfies  $\mathbf{x} \cdot \mathbf{k} = 0$ .



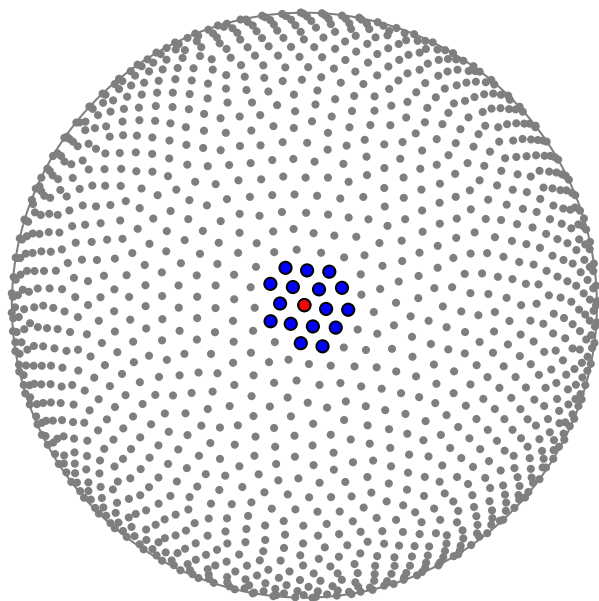
**Sample local directions**

\*Projections only fully cancel in the absence of currents or bathymetry variations.

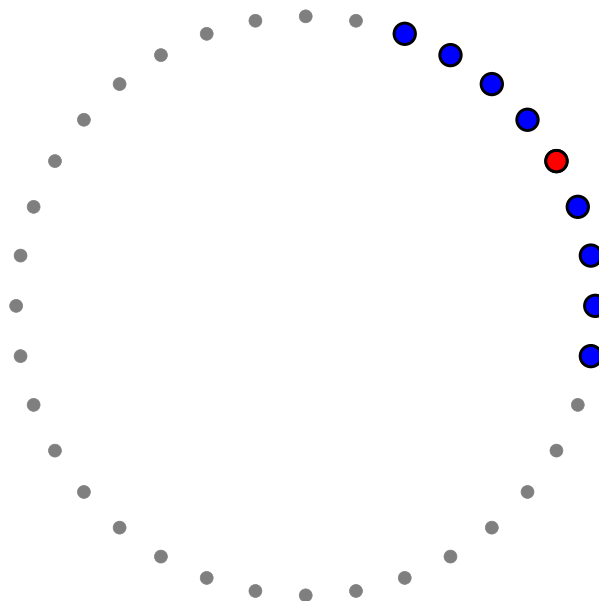
## V. Numerical method and directional alignment

- Approach tested with RBF-FD, a finite difference method on unstructured nodes.
  - Directional alignment of the nearest neighbors is defined by their projection onto the local tangent plane for the stencil node.
- 
- PHS+Poly scheme is used to avoid parameter tuning and add stability near boundaries.
  - Differential weights are assembled per spatial and directional node using nearest neighbors.
  - Wave spectral density for the desired projected direction is interpolated at each neighbor to estimate spatial advection in the same fixed direction.

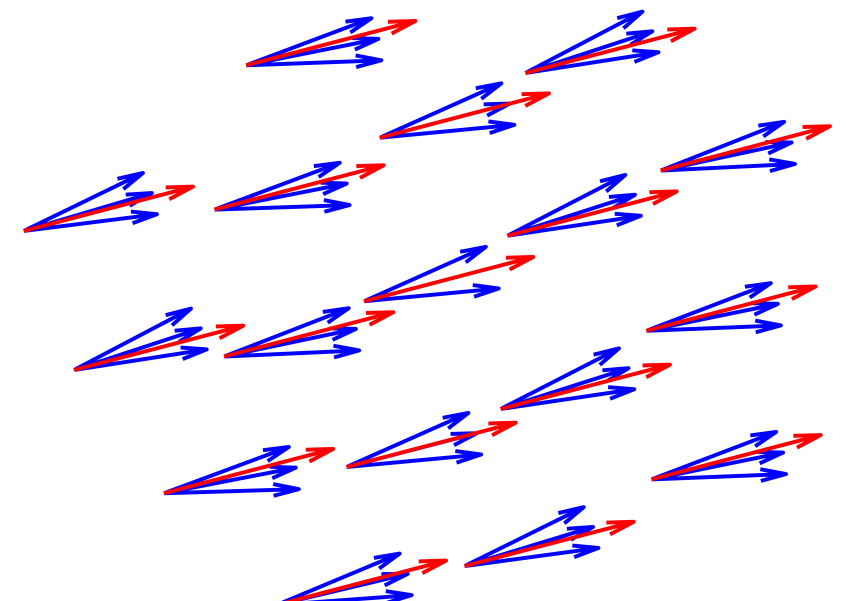
**Spatial stencil**



**Directional stencil**

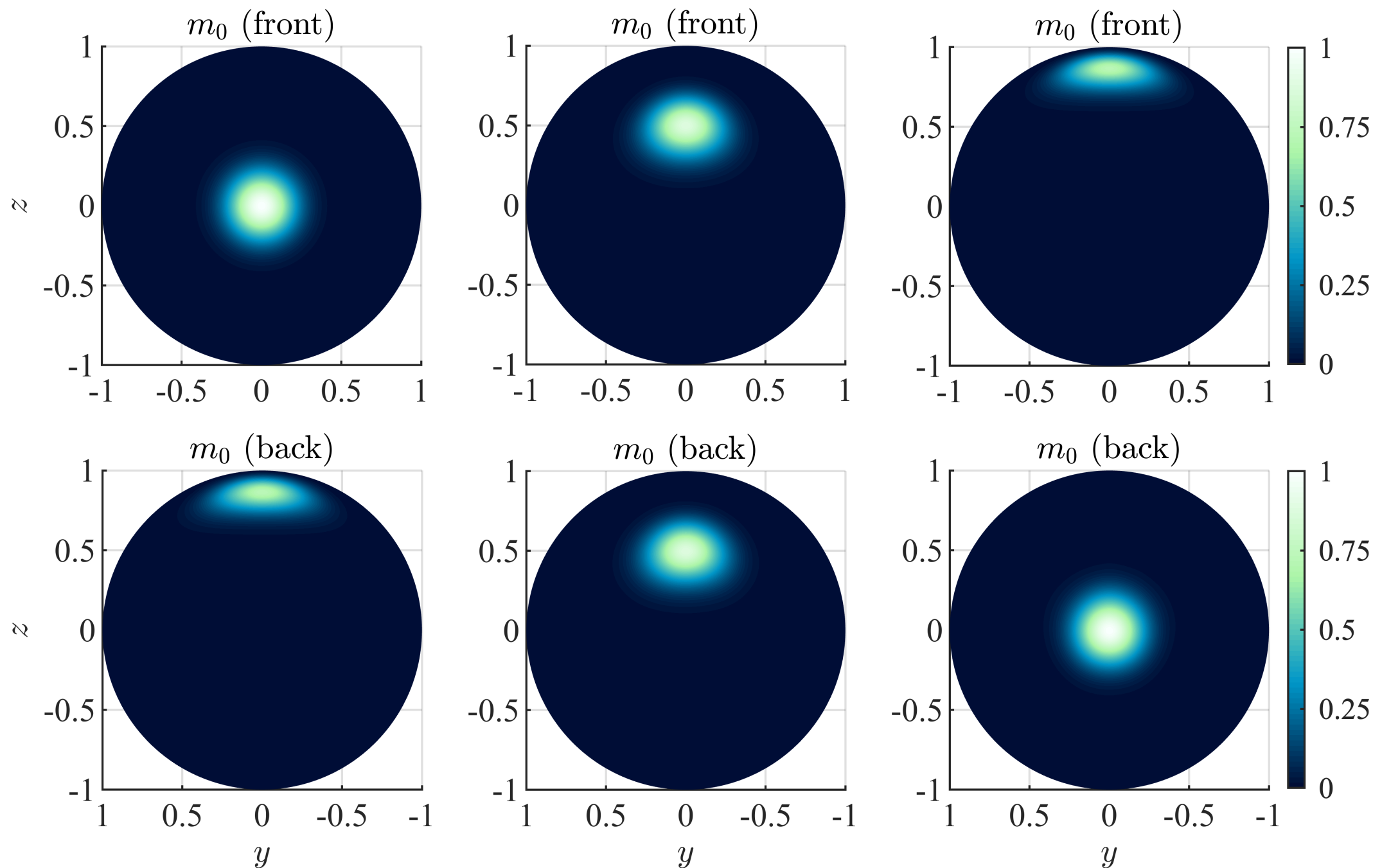


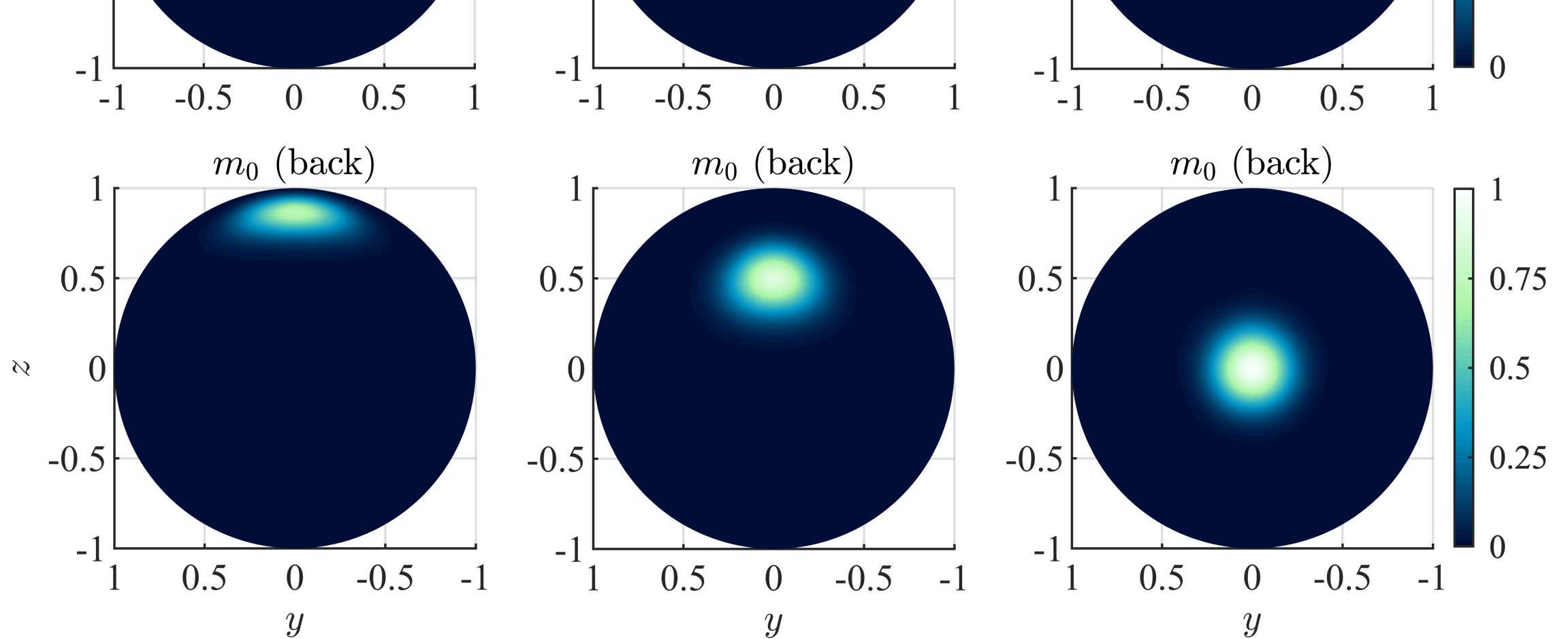
**Interpolated direction**



## VI. Results: Propagation across North Pole

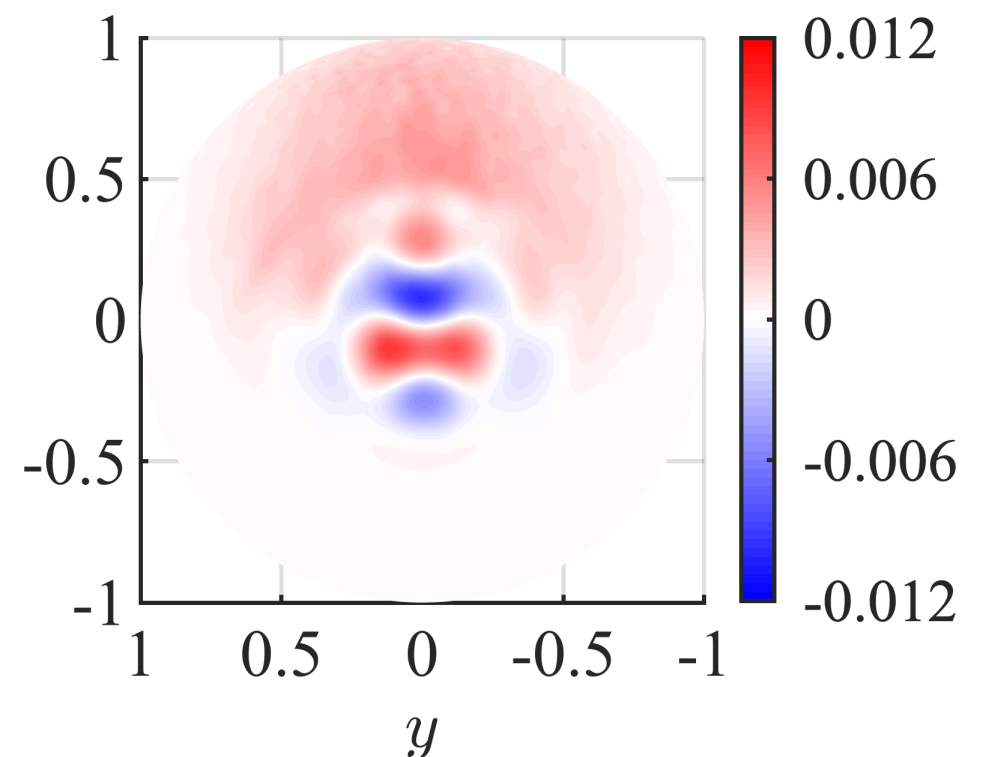
- Initial spatial amplitude: Normalized Gaussian bell (half-width  $20^\circ$ ) centered at  $(1,0,0)$ .
- Initial spectral distribution: Narrow cosine-power distribution (exponent = 20,  $\approx 60^\circ$  width) with an initial dominant direction of  $(0,0,1)$  at spatial bell center.





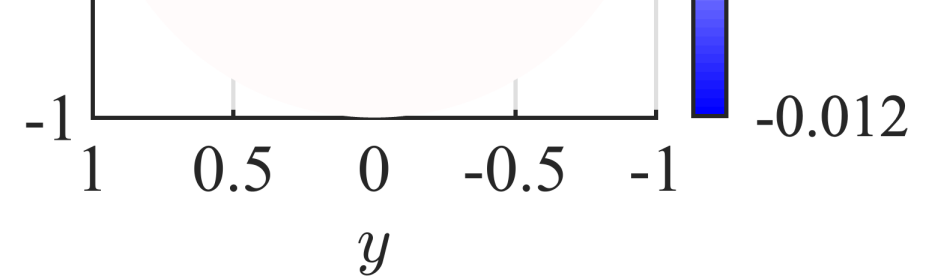
**Sample transport of a storm wave system across the North Pole. Zeroth moment ( $m_0$ ) shown at the following intervals:  $(0,1,2,4,5,6) T/6$ .**

- Relative residual error after 1/2 revolution shown.
- Model resolution:  $4^\circ$  spatial ( $N_x = 8100$ ,  $n_x = 31$ ),  $6^\circ$  directional ( $N_\theta = 60$ ,  $n_\theta = 9$ ,  $p_\theta = 5$ ).
- Similar errors obtained for different initial directions.
- WAVEWATCH III reference error:  $\approx 4\%$  for global  $1^\circ \times 1.25^\circ$  lat-lon model setup ( $N_x = 44000$ ,  $N_\theta = 36$ ).





- WAVEWATCH III reference error:  $\approx 4\%$  for global  $1^\circ \times 1.25^\circ$  lat-lon model setup ( $N_x = 44000$ ,  $N_\theta = 36$ ).



## References

- Flyer, N. and Wright, G. B., 2009. A radial basis function method for the shallow water equations on a sphere. *Proceedings of the Royal Society A*, 465(2106):1949–1976.
- Flyer, N., Fornberg, B., Bayona, V., and Barnett, G. A., 2016. On the role of polynomials in RBF-FD approximations: I. Interpolation and accuracy. *J. of Comp. Physics*, 321:21–38.
- Fuselier, E.J., Wright, G.B., 2013. A High-Order Kernel Method for Diffusion and Reaction-Diffusion Equations on Surfaces, *Journal of Scientific Computing*, 56:535–565.
- Group, T. W., 1988. The WAM Model—A Third Generation Ocean Wave Prediction Model. *Journal of Physical Oceanography*, 18(12):1775–1810.
- Gunderman, D., Flyer, N., and Fornberg, B., 2020. Transport schemes in spherical geometries using spline-based RBF-FD with polynomials. *J. of Comp. Physics*, 408:109256.
- Komen, G.J., Cavaleri, L., Donelan, M., et al., 1994. *Dynamics and Modeling of Ocean Waves*. Cambridge University Press, Cambridge, UK.

Research and travel funding supported by the Institute of Science Tokyo and Kakenhi Japan.

## Acknowledgements

